

Comparative analysis of cationic dye adsorption efficiency of thermally and chemically treated Tanzanian kaolin

Laurance Erasto

Government Chemist Laboratory Authority

Harieth Hellar-Kihampa (✉ hhellar@yahoo.co.uk)

The Open University of Tanzania <https://orcid.org/0000-0002-6951-5243>

Quentin Alphonse Mgani

College of Natural and Applied Sciences, University of Dar es Salaam

Esther Hellen Jason Lugwisha

College of Natural and Applied Sciences, University of Dar es Salaam

Research Article

Keywords: Clay modification, thermal and chemical treatment, adsorption efficiency, cationic dyes, Tanzanian kaolin

Posted Date: March 23rd, 2022

DOI: <https://doi.org/10.21203/rs.3.rs-1359298/v1>

License: © ⓘ This work is licensed under a Creative Commons Attribution 4.0 International License. [Read Full License](#)

Version of Record: A version of this preprint was published at Environmental Earth Sciences on February 8th, 2023. See the published version at <https://doi.org/10.1007/s12665-023-10782-w>.

Abstract

The effectiveness of thermal and acid modified locally available kaolin clay in Tanzania (Pugu clay), for removal of cationic dye from water systems were tested. The raw Pugu kaolin (RPK) was thermally-treated at 150°C for 7 hours and acid-leached with 0.2 M H₂SO₄ under reflux for 3 hours, to obtain thermally-activated Pugu kaolin (TAPK) and acid-activated Pugu kaolin (AAPK), respectively. The raw and modified clays were characterized by XRF, XRD, ATR-FTIR and Porosimeter for their mineralogical compositions, chemical compositions, specific surface areas and pore sizes. A comparative analysis of their respective adsorption efficiencies was carried out using basic blue 9 dye (BB9) as a representative adsorbate. The results revealed that while RPK was mainly composed of 44.18% silica and 26.70% alumina, the modified adsorbents had higher silica content of 46.95% and 58.81%; decreased alumina content of 24.11% and 12.74%, and increased surface areas from 15.36 to 41.07 m²/g and 149.61 m²/g, for TAPK and AAPK, respectively. Batch adsorption analysis indicated that AAPK and TAPK exhibited respective adsorption efficiency of 99.91% and 98.73% against BB9, compared to 96.82% of RPK. The Langmuir and Freundlich models with correlation coefficients close to unity indicated that the surface of the adsorbents were homo-heterogeneous in nature and exhibited mono-multilayer BB9 adsorption. This study has revealed that both raw and modified Pugu kaolin have good adsorption efficiency as ideal adsorbents in removal of cationic dyes from polluted water. Moreover, acid-activation resulted into a more effective adsorbent than thermal treatment.

1.0 Introduction

Studies have shown that clays can contribute significantly to environmental protection through refined removal of different chemical species in aqueous media. With more than 1,000,000 tonnes of dyes produced annually in the world, of which about 20% of it is lost to effluents during processing and use (Arora 2014), colored wastewater is a significant contributor to water pollution and an environmental concern. Dye-contaminated effluents are highly toxic enough to cause adverse effects to humans and the environment (Berradi et al. 2019), therefore their removal to acceptable levels before discharge into the environment is important. The applicability of diverse kinds of kaolin clays as adsorbent materials for this purpose has been widely researched and documented (e.g., Caponi et al. 2017; Bentahar et al. 2019; España et al. 2019; Behnamfard et al. 2019; Aragaw and Angerasa 2020; Malima et al. 2021). Researchers have also worked on clay modifications as a proven way of altering their vital properties so as to enhance their efficiency.

Modified clays have shown increased potential in removal of different organic and inorganic contaminants such as heavy metals, antibiotics, aromatics and various dyes (Han et al. 2019; Avila et al. 2021). Several chemical and physical modification methods have been employed in this context, including surfactant, alkaline activation, hybridization, thermal treatment and acid activation (e.g., Mudzielwana et al. 2019; David et al. 2020; Jawad and Abdulhameed 2020; Gil et al. 2021; Zaini et al. 2021). Thermal treatment is a physical modification method that involves heating the clay at a given temperature and duration to remove attached water moisture and impurities, hence exposing the adsorptive sites, and increasing the surface area (España et al. 2019). Acid activation as a chemical modification method, involves dissolution of the clay in a hot solution of a mineral acid such as sulfuric or hydrochloric acid, with expected results of increased specific surface area, porosity, surface acidity and catalytic activities (Dim and Termtanun 2021).

The highly versatile Pugu kaolin clay is widely available in a large deposit at Pugu, Kisarawe District, Coast Region, south west of Dar es Salaam city in Tanzania. Its relevance in various industrial and environmental uses, including wastewater treatment, has raised much interest (e.g., Kimambo et al. 2014; Lugwisha and Siafu 2014). In this study, the basic blue 9 dye (BB9) was used as a representative adsorbate to compare efficiency enhancement by the two modification methods, i.e., thermal treatment and acid activation, of the local clay in adsorbing cationic dye from contaminated water. The BB9, also known as methylene blue, is a tetra-methylthionine chloride compound with molecular formula C₁₆H₁₈ClN₃S·3H₂O, a molar mass of 373.90 g mol⁻¹, and colour index of 510152. It is used in medical procedures, pharmaceutical and textile industries. Although the dye is relatively less hazardous, it is still associated with several potential harmful effects, including breathing problems, diarrhea, nausea, headache, gastritis, increased heartbeat, jaundice, mental confusion and chest pain (Safae et al. 2018). Its high molecular weight allows it to accumulate in water bodies, thus reducing their luminosity, photosynthetic activity as well as the amount of dissolved oxygen, (Zhu et al. 2018).

In this comparative analysis, the raw Pugu kaolin clay (RPK) was first characterized to establish its mineralogical and chemical compositions, then its performance efficiency in adsorption of BB9 in aqueous environment was tested. The two modified versions of the RPK were prepared through thermal treatment to obtain thermal activated Pugu kaolin (TAPK) and acid activation to obtain acid activated Pugu kaolin clay (AAPK). Their properties were then investigated and compared, focusing on alterations in their mineralogical and chemical compositions and their absorbance efficiencies. The adsorption isotherms and kinetic mechanisms of the raw and modified clays were also investigated through a series of batch adsorption experiments.

2.0 Materials And Methods

2.1 Chemicals, reagents and equipment

All the chemicals used in this study were of analytical grade obtained from certified chemical suppliers. The chemicals included sodium hydroxide (NaOH) of assay 99% obtained from Blulux Laboratories (P) Ltd; hydrochloric acid (HCl) of assay 37% and hydrogen peroxide (H₂O₂) of assay 30% obtained from Scharlau Chemie SA, Spain; sulphuric acid (H₂SO₄) of assay 98% obtained from Fisher Scientific, UK; barium chloride (BaCl₂) of assay 98% obtained from J.T. Baker Chemical Company, U.S.A.; trihydrated basic blue dye (BB9) (C₁₆H₁₈ClN₃S·3H₂O) of assay 85% obtained from UNI-CHEMI and distilled water prepared at the Chemistry Department, University of Dar es Salaam. The instruments used in this study included alpha ATR-FTIR spectrometer (model: Bruker Optic GmbH 2011, U.S.A), X-ray powder diffractometer (model: BTX 231, inxitu inc., U.S.A), Nova 1200e Porosimeter (surface area and pore size analyzer, model: N12-28E, Quantachrome Corporation, Japan) and UV-Vis spectrophotometer (Analytikjena SPECORD 210 PLUS – 223F1376), all of them obtained at the Department of Geosciences, School of Mines and Geosciences, University of Dar es Salaam and an X-Ray Fluorescence spectrometer (model: S8 Tiger-SN. 206548, Bruker AXS company, Germany) obtained at the African Minerals and Geosciences Centre, Kunduchi, Dar es Salaam.

2.2 Preparation of the raw and modified clays

The raw clay sample used in this study was collected from the Pugu clay deposit located at latitude and longitude 6° 52' 29" South and 39° 2' 48" East, respectively in Kisarawe District, Coast Region, about 25 km from Dar es Salaam city. The raw kaolin clay lumps were air dried, crushed, and grinded with mortar and pestle, then sieved through a 300 µm sieve. The resulting fine powdery kaolin was soaked with hydrogen peroxide solution overnight, then washed with distilled water several times, followed by decantation and vacuum filtration to remove impurities. The resulted kaolin residue was then air dried in an oven at 100 °C for 12 hours and re-sieved by a 300 µm sieve to obtain the RPK, which was stored in an airtight plastic container for further experiments.

Thermal treatment of the RPK to obtain the TAPK was achieved through calcination of the RPK at 150 °C temperature for 7 hours in a muffle furnace, cooling it to room temperature for 3 hours in a desiccator and then put it in an airtight plastic container awaiting further use in adsorption studies. The acid activation of the RPK to obtain the AAPK was achieved by first calcinating the RPK at a temperature of 750 °C for 7 hours, then cooling it to room temperature. About 50 g of the calcined, cooled clay was then acid leached with 500 mL of 0.2 M sulfuric acid solution at 100 °C under reflux condition with constant stirring for 3 hours. The resulting suspension was washed with distilled water several times, followed by vacuum filtration to the point that filtrate did not form precipitates of BaSO₄ with barium (Ba²⁺) solution, that is neutral point. The resulting residues were then air dried in the oven at 100 °C for 12 hours, cooled to room temperature for 3 hours and re-sieved by 300 µm, then stored in airtight plastic container.

2.3 Characterization of the raw and modified clays

Instrumental characterization was performed on the RPK, TAPK and AAPK to identify their functional groups, mineralogical compositions, chemical composition and porosity. Functional groups were determined by ATR-FTIR spectrometer by analysing small amount of fine powder samples in the range of 400–4000 cm⁻¹ wave numbers. Mineralogical compositions were characterized by BTX 231 X-Ray powder diffractometer (under operating conditions of -45 °C, 30.03 kV, and 0.30 mA) connected to a computer with X Powder software. About 20 mg of homogeneous fine powder (150 µm particle size) of adsorbent sample were placed into the instrument, from which d-spacing values were determined within the position range of 5-55° 2θ. Elemental compositions of the raw and the modified clays defined by the major oxides, were determined by S8 Tiger XRF spectrometer with power of 5.2 kVA. About 10 g of fine powder of each sample were mixed with few drops of boric acid, a binding agent, then compressed into circular pellets of 34 mm diameter. The sample pellets were separately introduced into the sample tray of the instrument for analysis of both quantitative and qualitative elemental composition of the samples. Surface areas and pore sizes were analysed by a Nova 1200e Porosimeter using a nitrogen adsorption-desorption technique at 77.35 K and relative pressure in the range of 0.05 and 0.35. The porosimeter was connected to a computer with NovaWin software installed in it for measurement of surface area, pore size and pore diameter. About 0.1 g of each of the three fine powdery samples were first degassed at 160 °C to remove previously physisorbed contaminants. Then each sample was allowed to interact with liquid nitrogen for adsorption-desorption analysis, from which respective surface area, pore volume and diameter of the samples were obtained.

2.4 Preparation of the adsorbate

The standard stock solution of BB9 of 1 g/L concentration was prepared by dissolving 0.69 g BB9 powder in distilled water to make 0.5 L of a deep blue solution. The solid powder dye was first dissolved in small amount of distilled water, followed by addition of more water to the mark of the 500 mL flat bottomed volumetric flask, then thoroughly mixed. The resulting adsorbate solution was then stored away from light in the plastic bottles for preparation of the working solutions that were used in the adsorption studies. These were prepared in the concentration range of 0.1–100 mg/L by diluting the stock solution based on the dilution law equation: $C_i V_i = C_d V_d$, whereby a given amount of distilled water was added to an initial volume V_i with concentration C_i of the stock solution to make new volume V_d of dilute working solution with desired concentration C_d .

2.5 Batch adsorption experiments

2.5.1 Pre-adsorption studies

Adsorption studies were preceded by the determination of optimal wavelengths for the BB9, preparation of calibration curves for the adsorbate as well as determination of the pH at the Zero Point of Charge (pH_{ZPC}). Maximal absorbance for BB9 was measured by Analytikjena SPECORD 210 PLUS UV-Vis spectrophotometer. About 3 mL of standard solutions (2.50, 3.00 and 3.50 mg/L of BB9) were placed in the cuvette, and then introduced into the instrument for determination of maximum absorbances corresponding to the respective optimal wavelengths. The optimal wavelengths were determined through spectral scan mode within the visible region (350–800 nm). These optimal wavelengths were then used in the measurements of the maximum absorbances in the determination of the BB9 calibration curve as well as various supernatants obtained in the course of adsorption studies. Several standard solutions of BB9 in the range of 0.1–6.0 mg/L at pH of 6.81 and temperature of 27 °C were prepared, followed by measurements of respective maximum absorbance by UV-Vis spectrophotometer at the predetermined optimal wavelength of 665 nm. A linear plot of absorbance against concentration was obtained based on the Beer-Lambert's law equation:

$$A = \epsilon lc$$

Where: A = absorbance; l = path length (cm); c = concentration of solution (mol/L) and ϵ = Molar absorptivity (L mol⁻¹ cm⁻¹). The plots were used to determine respective free or equilibrium concentration of each adsorbate dye available in the adsorbent-adsorbate system after given contact time.

To determine the pH at the Zero Point of Charge (pH_{ZPC}), ten samples of RPK of 0.5 g each and particle size of 300 µm, were mixed with 0.05 L of distilled water of known initial pH in the range of 2–11. Adjustment of pH was attained by addition of few drops of either dilute HCl or NaOH. The systems (water-RPK

mixture) were shaken for 12 h at 27 °C to attain final equilibrium pH. The initial and final pH of each system was measured by digital pH meter. Thereafter determination of the pH_{ZPC} was made from the plot of final pH against initial pH.

2.5.2 Adsorption Studies

Batch adsorption technique was used to investigate the effects of temperature, adsorbent dose, initial pH of adsorbate solution, contact time and initial adsorbate concentration on adsorption efficiency of RPK, TAPK and AAPK adsorbents; with batch volume of 0.05 L, pH of 6.80, particle size of 300 μ m, adsorbate concentration of 30 mg/L and mass of 0.5 g of adsorbents. The system was maintained at 26.5 °C and shaken for 3 h. The adsorption capacity (q_e) of adsorbent and adsorption efficiency (A_e) at equilibrium was determined based on the equations 1a and 1b below, respectively (Nandi et al. 2009; Adeyemo et al. 2017).

$$q_e = (c_i - c_e) * v/m \dots\dots(1a)$$

$$A_e (\%) = (c_i - c_e) * 100/c_i \dots\dots(1b)$$

Where: q_e = amount of adsorbate adsorbed per unit mass of adsorbent at equilibrium (mg/g), A_e (%) = adsorption efficiency, c_i = initial dye concentration (mg/L), v = volume of solution (L) and m = dry mass of kaolin adsorbent (g), and c_e = adsorbate concentration (mg/L) at equilibrium.

The effect of temperature on adsorption was investigated at temperatures of 27, 43, 56, 76 and 90 °C; while the effect of adsorbent dose was investigated with adsorbent doses of 0.1, 0.3, 0.5, 0.7 and 0.9 g, and the effect of initial pH of adsorbate solution was studied with initial pH of 3, 5, 7, 9 and 11. Furthermore, the effect of contact time was investigated at contact time of 20, 60, 100, 140 and 180 minutes; while the effects of concentration on adsorption was studied at initial concentration of 30, 45, 60, 75 and 90 mg/L. In all cases, each adsorbate-adsorbent system was centrifuged to obtain respective supernatants for analysis of respective equilibrium concentration of BB9, from which respective adsorption efficiency of RPK, TAPK and AAPK adsorbent was determined.

The Freundlich and Langmuir models were used to test the nature of adsorption isotherms for the adsorbate-adsorbent systems in this study, based on the equations 2 and 3:

$$\ln q_e = \ln K_f + (1/n) \ln c_e \dots\dots\dots (2) \text{ (Singh 2016)}$$

Where q_e is the amount of adsorbate adsorbed per unit mass of adsorbent at equilibrium (mg/g); c_e is equilibrium concentration of the adsorbate dye (mg/L); $1/n$ is the measure of adsorption intensity and K_f is the Freundlich constant that define measure of adsorption capacity.

$$c_e/q_e = 1/bq_m + c_e/q_m \dots\dots\dots (3) \text{ (Liu et al. 2019).}$$

Where b is the Langmuir constant (L/mg); q_e is the quantity of adsorbate adsorbed per unit adsorbent mass (mg/g); c_e is the equilibrium concentration of adsorbate (mg/L) and q_m is the maximum adsorption capacity (mg/g). Additionally, the constant b from the equation above is used in determination of the was used to determine separation factor $S_f = 1/(1 + bc_e)$; whose value is significant for prediction of favorability and reversibility of the adsorption process: $S_f = 0$ describe irreversible adsorption, $S_f = 1$ represent linear adsorption, $0 < S_f < 1$ indicate favorable and linear adsorption, and $S_f > 1$ indicate unfavorable adsorption (Sharma 2015; Rahman et al. 2015; Boukhemkhem and Rida 2017).

3.0 Results And Discussion

3.1 Characteristics of the raw and modified adsorbents

3.1.1 Functional Groups

Figure 1 compares the ATR-FTIR spectra for RPK, TAPK and AAPK. It shows that RPK exhibited absorption peaks at 788.67 and 752.92 cm^{-1} and sharp peaks at 3687.28 and 3619.17 cm^{-1} corresponding to pure and crystalline kaolinite respectively (Olaremu 2015). In addition, the peaks at 1004.86, 911.73, 688.06, 533.44 and 462.37 cm^{-1} also suggested the presence of kaolinite in the sample. Similar observations have been also reported in other research studies (Sejie and Nadiye-Tabbiruka 2016; Boukhemkhem and Rida 2017). The TAPK adsorbent exhibited comparable ATR-FTIR absorption bands with RPK. Such resemblance anticipated that there were no significant structural changes of RPK upon thermal activation. The major peaks observed correspond to the wave numbers: 3686.77, 3619.25, 1004.24, 911.42, 788.87, 752.98, 687.87, 532.92 and 461.48 cm^{-1} . However, the peaks were relatively more intense than those of RPK; implying that some impurities have been removed upon calcination of RPK at 150 °C resulting into surface modification with increased exposure of adsorptive sites. The absence of absorption band at 1638.17 cm^{-1} implies that physisorbed hydration water molecules have been removed (Kumar et al. 2013) during the calcination process of the RPK.

The AAPK adsorbent exhibited different ATR-FTIR spectrum from RPK and TAPK. The peaks have been either reduced, shifted, disappeared or new band emerged. As case study, the 3687.24 and 3619.38 cm^{-1} bands have been transformed into broad peak and shifted to bands of 3372.92 cm^{-1} ; while 752.92 cm^{-1} has shifted to 724.56 cm^{-1} band, and 688.06 cm^{-1} shifted to 645.75 cm^{-1} peak. Furthermore, 533.44 cm^{-1} sharp peak has transformed into broad peak at 581.53 cm^{-1} with reduced intensity. On the other hand, 426.80, 911.73 and 1004.86 cm^{-1} peaks disappeared while new peak at 1076.11 cm^{-1} have been emerged during thermal acid activation of RPK. The new peak proposed the presence of amorphous silica. The observations made reflected structural and

surface modification hence loss of crystalline nature of the kaolinite in RPK sample. Such observation is in good agreement with other findings (e.g., Gao et al. 2016).

Table 1 compares the absorption bands (cm^{-1}) before and after adsorption of BB9. It shows that almost all absorption bands remained the same before and after adsorption but with reduced intensities after adsorption. Such observations imply that physisorption between RPK, TAPK and AAPK adsorbents and BB9 adsorbate predominated. The decreased peak intensities of RPK, TAPK and AAPK suggested that exposure of the respective adsorbent functional groups has been reduced as results of BB9 adsorption. The observation is closely related to the ones reported in other research works (e.g., Shuma et al. 2019).

Table 1: Absorption Bands (cm^{-1}) before and after Adsorption of BB9

System	-OH Stretching	-OH Stretching	H-O-H Stretching	Si-O-Si, Si-O Stretching	Al-Al-O, Al-OH Stretching	Si-O, Si-O-Al, (Al, Fe, Mg)-OH, Si-O-Si (Stretching)	Si-O-Al Bending	Si-O, Si-O-Al Stretching	Si-O, Si-O-Al Stretching	Si-O, Si-O-Fe Stretching	Si-O Bending
RPK	3687.2	3619.4	1638.2	1004.9	911.7	788.7	752.9	688.1	533.4	462.4	426.8
RPK-BB9	3689.8	3619.2	1634.7	1006.4	911.5	786.6	753.1	690.2	534.9	464.1	428.2
TAPK	3686.8	3619.3	-	1004.2	911.4	788.9	753.0	687.9	532.9	461.5	426.8
TAPK-BB9	3687.1	3619.2	1739.3	1006.2	911.6	787.1	751.5	692.1	534.6	462.8	428.7
AAPK	3372.9	-	1635.8	1076.1	-	783.4	724.6	645.8	581.5	461.8	-
AAPK-BB9	3344.7	-	1634.6	1076.7	-	778.5	727	647.7	582.3	463.9	-

3.1.2 Mineralogical compositions of the adsorbents

The XRD patterns from the three clay versions (Figure 2) shows that RPK identified kaolinite [$\text{Al}_2\text{Si}_2\text{O}_5(\text{OH})_4$], a clay material phase as well as quartz (SiO_2) and potassium feldspar (microcline) [KAlSi_3O_8] as impurities in the kaolin sample. The raw kaolin used in this study was composed largely of crystalline kaolinite with coarser grains, as well as microcline and quartz (Kimambo et al. 2014). Furthermore, the resemblance of TAPK pattern to that of RPK suggested that there were no significant structural changes upon thermal activation of the RPK. However close analyses exemplify a slight decrease in intensity of kaolinite peaks for TAPK accounting for decreased crystallinity. On the other hand, complete loss of the same major peaks of 7.16 and 3.58 Å for AAPK indicated loss of kaolinite in the sample upon acid activation.

The presence of tridymite silica and disappearance of kaolinite phase for the AAPK pattern accounts for surface and structural changes resulted from calcination reaction of the kaolin clay at 750 °C and acid leaching of the RPK. Both calcination and acid leaching resulted into a powderier amorphous Kaolin with increased silica content. These findings are in good agreement with those reported by other researchers (e.g., Boukhemkhem and Rida 2017; Luo et al. 2017). The results also correlate well with the observed decreased percent composition of Al_2O_3 and increased silica (SiO_2) content from the XRF analysis.

3.1.3 Chemical compositions of the adsorbents

Table 2 summarizes the chemical compositions of the adsorbents defined by the major oxides. It shows that RPK was mainly composed of silica (SiO_2) - 44.18% and alumina (Al_2O_3) - 26.7%. These results are in good agreement with that reported by Akwilapo and Wiik (2004). The TAPK and AAPK adsorbents exhibited increased silica content to 46.95% and 58.81%, and decreased alumina content to 24.11% and 12.74%, respectively after modification. In AAPK, the alumina and iron oxide (Fe_2O_3) decreased much more, probably due to the effect of acid leaching of the previously calcined kaolin, due to the equation:



Table 2: Elemental compositions of RPK, TAPK and AAPK adsorbents

Composition (%)	SiO_2	Al_2O_3	Fe_2O_3	CaO	MgO	K_2O	Na_2O	SO_3	MnO	P_2O_5	LOI
RPK	44.18	26.70	1.78	13.01	0.54	1.73	0.04	0.04	0.02	0.06	11.90
TAPK	46.95	24.11	1.49	14.36	0.29	1.59	0.07	0.07	0.03	0.08	10.96
AAPK	58.81	12.74	0.82	14.53	0.12	1.87	0.07	0.03	0.05	0.08	10.88

The other oxides also showed changes in percentage compositions of TAPK and AAPK compared to RPK e.g., decrease in Fe_2O_3 and MgO, and increase in CaO, Na_2O and MnO, which inferred to the structural and surface modification resulting from thermal and acid activation. Such changes have also been reflected by XRD diffractograms as well as FTIR spectra in this study. Similar effects of the thermal and acid treatment on kaolin have been also reported in other studies (e.g., Gao et al. 2016; Boukhemkhem and Rida 2017).

3.2 The effects of operating parameters on adsorption efficiency

Figure 3(a – e) summarizes the results of the effects the operating parameters on adsorption efficiency, i.e., temperature, adsorbent dose, contact time, initial concentration and initial pH on adsorption of the BB9 dye by the raw and modified adsorbents.

The graph in Figure 3(a) shows that the adsorption efficiency and quantity adsorbed per unit mass of adsorbent decreased as temperature was raised from 27 to 90 °C in the order: RPK (81.45 to 61.58%) < TAPK (89.43% to 76.40%) < AAPK (96.62% to 81.23%). Such observation implies that the adsorption processes were exothermic in nature and more favorable at low temperature. The variation in adsorption efficiency was also proportional to the surface area of the adsorbents that increased in the order of AAPK > TAPK > RPK. With respect to adsorbent dose (Figure 3b), the adsorption efficiency decreased in the order of AAPK (69.54 to 99.74%) > TAPK (49.23 to 98.73%) > RPK (40.82 to 96.82%); as adsorbent dose increased from 0.1, 0.3, 0.5, 0.7 to 0.9 g. The increased adsorbent dose account for increased adsorptive sites and surface area hence increased adsorption efficiency (He et al. 2019).

Figure 3(c) also shows that adsorption efficiency increased with contact time from 0, 20, 60, 100, 140 to 180 minutes in the trend of 83.59%, 94.00%, and 99.25% for RPK, TAPK and AAPK, respectively. The rate of adsorption was much faster within the first 20 min. Thereafter percent colour removal increased slowly to about equilibrium within contact time of 180 min. The higher adsorption rate in the first few minutes of contact time accounts for availability of enough free adsorptive sites as well as surface area of the adsorbents. Later on, the number of free adsorptive sites and surface area decreased with increased contact time accounting for the observed slower adsorption rate. Similar observations of the adsorption behaviour of kaolin as a function of contact time have also been reported by Lugwisha and Lunyungu (2016).

The adsorption efficiency of BB9 increased from 68.71 to 94.73% for RPK, 78.63 to 97.37% for TAPK and 94.13 to 98.85% for AAPK as initial adsorbates pH increased from 3, 5, 7, 9 and 11 (Figure 3e). The higher BB9 adsorption likely was due to the increased electrostatic interaction between cationic BB9 and adsorbents arising from increased strength of the negative charge on respective adsorbents as pH increased. Similar observations have also been reported by other researchers (e.g., Mustapha et al. 2019). On the other hand, the percent of colour removal decreased with increased initial adsorbate concentration from 30, 45, 60, 75 to 90 mg/L. This is due to the fact that, the system with initial higher concentration exhibited higher equilibrium concentration than system with initial lower concentration at constant number of adsorptive sites as well as surface area and contact time. This possibly suggests more contact time and adsorbent dose are required under condition of initial high concentration of adsorbates for effective colour removal.

3.3 Adsorption Isotherm

Figure 4 depicts the Freundlich and Langmuir adsorption isotherms parameters. The Freundlich isotherm exhibited correlation coefficient $R = \sqrt{R^2}$ values of 0.995, 0.994 and 0.949 for RPK, TAPK and AAPK-BB9 adsorption systems, respectively. These values approaching unit, together with values of adsorption intensity (n) in the range of 2-10 suggested favourable multilayer adsorption of BB9 adsorbates onto heterogeneous adsorbent surface. It is also important to note that activated kaolins showed better adsorption than the raw kaolin as confirmed by respective higher values of adsorption intensity. Comparable findings have been reported by Boukhemkhem and Rida (2017). The fact that activated kaolins shows enhanced adsorption can also be deduced from increased values of adsorption capacity (K_f) in the order of AAPK > TAPK > RPK. The value of $1/n$ less than one generally indicates favourable adsorption process.

On the other hand, the Langmuir adsorption isotherms are linear with correlation coefficient R values of 0.991, 0.988 and 0.987 for RPK, TAPK and AAPK-BB9 systems, respectively. These R values together with values of separation factor S_f ($0 < S_f < 1$) suggested favorable monolayer adsorption as it has been also reported by Elmoubarki et al. (2015); Aguiar et al (2017) and Mustapha et al. (2019). The smaller value of S_f implies strong interaction between adsorbate and adsorbents which agree with observed higher adsorption rate and efficiency. Activated clays exhibited enhanced adsorption which agree with increased values of adsorption energy in the order of AAPK > TAPK > RPK. The enhanced adsorption of activated clays was in agreement with increased respective surface area that have been observed under this study.

Conclusion

Adsorption efficiencies of the thermally-treated and acid-activated Pugu kaolin clay against BB9 adsorbate, a cationic dye in aqueous environment, were compared. Instrumental characterization of the raw and modified kaolins revealed that the raw adsorbent which was mainly composed of silica and alumina resulted into adsorbents with higher silica content and lower alumina content upon modifications. The acid activated adsorbent showed the disappearance of the kaolinite phase and appearance of the tridymite phase due to structural changes. The XRF analysis also showed significant changes in the major elemental compositions of the modified adsorbents, confirming that the thermal and acid treatments resulted into structural and surface modifications. The surface areas of the raw adsorbent increased significantly upon modification, and was higher in the acid activated than the thermal treated adsorbent by more than 100 m²/g. This increased the adsorption of the BB9 dye by the modified kaolins by up to 4%. The operating parameters of temperature, contact time, initial pH of adsorbate, initial concentration of adsorbate and adsorbent dose were detected to affect the adsorption efficiency in terms of percent color and quantity of adsorbate adsorbed. The Langmuir and Freundlich adsorption isotherm models implied that the adsorption process was mono-multilayer in nature between BB9 adsorbates and the adsorbents. The Langmuir constant and the Freundlich constant increased in the order of acid-activated kaolin > thermally-treated kaolin > raw kaolin for both adsorption systems. Such trend indicated that the raw kaolin exhibited relatively weak interactions with adsorbates than the modified kaolins. Conclusively, the results from this study demonstrated that modification of the Pugu kaolin clay by both thermal treatment and acid activation significantly enhanced its capacity to remove cationic dyes from aqueous solutions. Moreover, acid activation resulted into an adsorbent with superior adsorption efficiency than thermal treatment.

Declarations

Acknowledgements

The contributions of the technical staff at the Department of Geosciences, School of Mines and Geosciences, University of Dar es Salaam and the African Minerals and Geosciences Centre, Kunduchi, Dar es Salaam in carrying out the instrumental analyses are highly appreciated

Funding

The authors declare that no funds, grants, or other support were received during the preparation of this manuscript.

Competing Interests

The authors declare that they have no known competing financial or personal interests that could have influence the work reported in this paper.

Author contributions

All authors contributed to the study conception and design. Laurance Erasto contributed in conceptualization, methodology, investigation and data curation. Harieth Hellar-Kihampa contributed in writing of the original draft and visualization. Quentin Alphonse Mgani contributed in conceptualization, methodology and supervision. Esther Hellen Lugwisha contributed in conceptualization, methodology, supervision and mentorship.

References

1. Adeyemo AA, Adeoye IO, Bello OS (2017) Adsorption of dyes using different types of clay: a review. *Appl Water Sci* 7:543–568. <https://doi.org/10.1007/s13201-015-0322-y>
2. Aguiar JE, Cecilia JA, Tavares PAS, Azevedo DCS, Rodríguez Castellón E, Lucena SMP, Silva IJ (2017) Adsorption study of reactive dyes onto porous clay heterostructures. *Appl Clay Sci* 135:35–44. <https://doi.org/10.1016/j.clay.2016.09.001>
3. Akwilapo LD, Wiik K (2004) Ceramic properties of pugu kaolin clays. Part 2: Effect of phase composition on flexural strength. *Bull Chem Soc Ethiop* 18:1–10. <https://doi.org/10.4314/bcse.v18i1.61631>
4. Aragaw TA, Angerasa FT (2020) Synthesis and characterization of Ethiopian kaolin for the removal of basic yellow (BY 28) dye from aqueous solution as a potential adsorbent. *Heliyon* 6:e04975. <https://doi.org/10.1016/j.heliyon.2020.e04975>
5. Arora S (2014) Textile Dyes: Its Impact on Environment and its Treatment. *J Bioremediat Biodegrad* 5:e146. <https://doi.org/10.4172/2155-6199.1000e146>
6. Avila MC, Lick ID, Comelli NA, Ruiz ML (2021) Adsorption of an anionic dye from aqueous solution on a treated clay. *Groundw Sustain Dev* 15:100688. <https://doi.org/10.1016/j.gsd.2021.100688>
7. Behnamfard A, Chegni K, Alaei R, Veglio F (2019) The effect of thermal and acid treatment of kaolin on its ability for cyanide removal from aqueous solutions. *Environ Earth Sci* 78:408. <https://doi.org/10.1007/s12665-019-8408-8>
8. Bentahar Y, Draoui K, Hurel C, Ajouryed S
9. Marmier N (2019) Physico-chemical characterization and valorization of swelling and non-swelling Moroccan clays in basic dye removal from aqueous solutions. *J Afr Earth Sci* 154:80–88. <https://doi.org/10.1016/j.jafrearsci.2019.03.017>
10. Berradi M, Hsissou R, Khudhair M, Assouag M, Cherkaoui O, El Bachiri A, El Harfi A (2019) Textile finishing dyes and their impact on aquatic environs. *Heliyon* 5(11):e02711. <https://doi.org/10.1016/j.heliyon.2019.e02711>
11. Boukhemkhem A, Rida K (2017) Improvement adsorption capacity of methylene blue onto modified tamazert kaolin. *Adsorp Sci Technol* 35(9–10):753–773. <https://doi.org/10.1177/0263617416684835>
12. Caponi N, Collazzo GC, Jahn SL, Dotto GL, Mazutti MA, Foletto EL (2017) Use of Brazilian kaolin as a potential low-cost adsorbent for the removal of malachite green from colored effluents. *Mater Res* 20:14–22. <https://doi.org/10.1590/1980-5373-MR-2016-0673>
13. David MK, Okoro UC, Akpomie KG, Okey C, Oluwasola HO (2020) Thermal and hydrothermal alkaline modification of kaolin for the adsorptive removal of lead(II) ions from aqueous solution. *SN Appl Sci* 2:1134. <https://doi.org/10.1007/s42452-020-2621-7>
14. Dim PE, Termatanun M (2021) Treated clay mineral as adsorbent for the removal of heavy metals from aqueous solution. *Appl Sci Eng Prog* 14(3):511–524. <https://doi.org/10.14416/j.asep.2021.04.002>
15. Elmoubarki R, Mahjoubi F, Tounsadi H, Moustadraf J, Abdennouri M, Zouhri A, El Albani A, Barka N (2015) Adsorption of textile dyes on raw and decanted moroccan clays: Kinetics, equilibrium and thermodynamics. *Water Resour Ind* 9:16–29. <https://doi.org/10.1016/j.wri.2014.11.001>
16. España VAA, Sarkar B, Biswas B, Rusmin R, Naidu R (2019) Environmental applications of thermally modified and acid activated clay minerals: Current status of the art. *Environ Technol Innov* 13:383–397. <https://doi.org/10.1016/j.eti.2016.11.005>
17. Gao W, Zhao S, Wu H, Deligeer W, Asuha S (2016) Direct acid activation of kaolinite and its effects on the adsorption of methylene blue. *Appl Clay Sci* 126:98–106. <https://doi.org/10.1016/j.clay.2016.03.006>
18. Gil A, Santamaría L, Korili SA, Vicente MA, Barbosa LV, de Souza SD, Marçal L, de Faria EH, Ciuffi KJ (2021) A review of organic-inorganic hybrid clay-based adsorbents for contaminants removal: Synthesis, perspectives and applications. *J Environ Chem Eng* 9:105808. <https://doi.org/10.1016/j.jece.2021.105808>
19. Han H, Rafiq MK, Zhou T, Xu R, Mašek O, Li X (2019) A critical review of clay-based composites with enhanced adsorption performance for metal and organic pollutants. *J Haz Mater* 369:780–796. <https://doi.org/10.1016/j.jhazmat.2019.02.003>

20. He K, Zeng G, Chen A, Huang Z, Peng M, Huang T, Chen G (2019) Graphene hybridized polydopamine-kaolin composite as effective adsorbent for methylene blue removal. *Compos B: Eng* 161:141–149. <https://doi.org/10.1016/j.compositesb.2018.10.063>
21. Jawad AH, Abdulhameed AS (2020) Facile synthesis of crosslinked chitosan-tripolyphosphate/kaolin clay composite for decolourization and COD reduction of remazol brilliant blue R dye: Optimization by using response surface methodology. *Colloids Surf A: Physicochem Eng* 605:125329. <https://doi.org/10.1016/j.colsurfa.2020.125329>
22. Kimambo V, Philip JYN, Lugwisha EHJ (2014) Suitability of Tanzanian kaolin, quartz and feldspar as raw materials for the production of porcelain tiles. *Int J Sci Technol Soc* 2:201–209. <https://doi.org/10.11648/j.ijsts.20140206.17>
23. Kumar S, Panda AK, Singh R (2013) Preparation and characterization of acid and alkaline treated kaolin clay. *Bull Chem React Eng Catal* 8:61–69. <https://doi.org/10.9767/bcrec.8.1.4530.61-69>
24. Liu L, Luo X, Ding L, Luo S (2019) Application of Nanotechnology in the Removal of Heavy Metal from Water. In: Luo X, Deng F (eds) *Micro and Nano Technologies, Nanomaterials for the Removal of Pollutants and Resource Reutilization*. Elsevier, Amsterdam, pp 83–147. <https://doi.org/10.1016/B978-0-12-814837-2.00004-4>
25. Lugwisha EHJ, Lunyungu G (2016) Water defluoridation capacity of Tanzanian kaolin-feldspar blend adsorbents. *Am J Appl Chem* 4:77–83. <https://doi.org/10.11648/J.AJAC.20160403.12>
26. Lugwisha EHJ, Siafu SI (2014) The properties of feldspathic dental porcelain from tanzanian aluminosilicate materials. *Int J Dev Res* 4:2260–2265. <http://dspace.nm-aist.ac.tz/handle/123456789/197>
27. Luo J, Jiang T, Li G, Peng Z, Rao M, Zhang Y (2017) Porous materials from thermally activated kaolinite: Preparation, characterization and application. *Materials* 10:647. <https://doi.org/10.3390/ma10060647>
28. Malima NM, Owonubi SJ, Lugwisha EHJ, Mwakaboko AS (2021) Development of cost-effective and eco-friendly adsorbent by direct physical activation of Tanzanian Malangali kaolinite for efficient removal of heavy metals. *Mater Today Proc* 38(2):1126–1132. <https://doi.org/10.1016/j.matpr.2020.06.469>
29. Mudzielwana R, Gitaria MW, Ndungu P (2019) Performance evaluation of surfactant modified kaolin clay in As(III) and As(V) adsorption from groundwater: adsorption kinetics, isotherms and thermodynamics. *Heliyon* 5(11):e2756. <https://doi.org/10.1016/j.heliyon.2019.e02756>
30. Mustapha S, Ndamitso MM, Abdulkareem AS, Tijani JO, Mohammed AK, Shuaib DT (2019) Potential of using kaolin as a natural adsorbent for the removal of pollutants from tannery wastewater. *Heliyon* 5(11):e02923. <https://doi.org/10.1016/j.heliyon.2019.e02923>
31. Nandi BK, Goswami A, Purkait MK (2009) Adsorption characteristics of brilliant green dye on kaolin. *J Haz Mater* 161:387–395. <https://doi.org/10.1016/j.jhazmat.2008.03.110>
32. Olaremu AG (2015) Physico-chemical characterization of Akoko mined kaolin clay. *J Min Mater Charact Eng* 3:353–361. DOI: <https://doi.org/10.4236/jmmce.2015.35038>
33. Rahman A, Kishimoto N, Urabe T (2015) Adsorption characteristics of clay adsorbents—sepiolite, kaolin and synthetic talc—for removal of reactive yellow 138. *Water Environ J* 29:375–382. <https://doi.org/10.1111/wej.12131>
34. Safae BL, Abdellah D, Mohammed EK, Noureddine EM, Abdellah L (2018) Removal of a cationic dye from aqueous solution by natural clay. *Groundw Sustain Dev* 6:255–262. <https://doi.org/10.1016/j.gsd.2018.02.002>
35. Sejie FP, Nadiye-Tabbiruka MS (2016) Removal of Methyl Orange (MO) from Water by adsorption onto Modified Local Clay (Kaolinite). *Phys Chem* 6(2):39–48. <https://doi.org/10.5923/j.pc.20160602.02>
36. Sharma SK (2015) *Green chemistry for dyes removal from waste water: Research trends and applications*. John Wiley & Sons, Inc., Hoboken, New Jersey
37. Shuma HE, Mkyula LL, Makame YMM (2019) Assessment of the Effect of Acid Activation of Kaolin from Malangali on Water Defluoridation. *Tanz J Sci* 45(2):279–296
38. Singh AK (2016) In: Singh AK, Nanoparticles E (eds) *Nanoparticle Ecotoxicology*. Academic Press, Cambridge, Massachusetts, pp 343–450. <https://doi.org/10.1016/B978-0-12-801406-6.00008-X>
39. Zaini NSM, Lenggoro IW, Naim MN, Yoshida N, Che Man H, AbuBakar NF, Puasa SW (2021) Adsorptive capacity of spray-dried pH-treated bentonite and kaolin powders for ammonium removal. *Adv Powder Technol* 32(6):1833–1843. <https://doi.org/10.1016/j.apt.2021.02.036>
40. Zhu C, Feng Q, Ma H, Wu M, Wang D, Wang Z (2018) Effect of Methylene Blue on the Properties and Microbial Community of Anaerobic Granular Sludge. *BioResources* 13(3):6033–6046

Figures

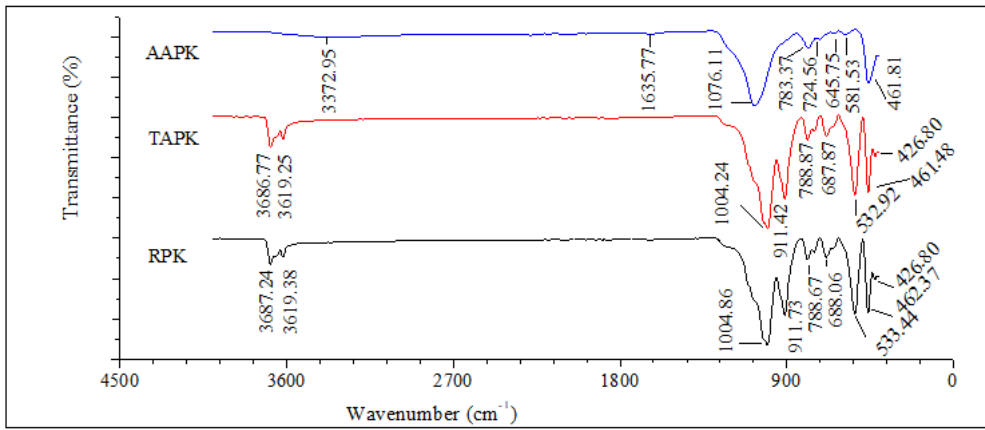


Figure 1

Comparative ATR-FTIR Spectra for RPK, TAPK and AAPK Adsorbent

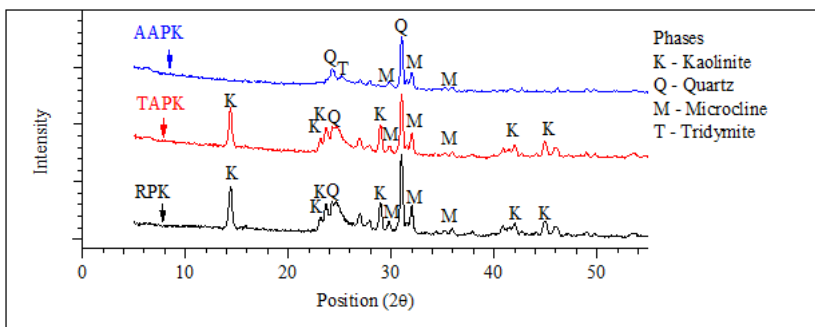


Figure 2

Comparative XRD Patterns for RPK, TAPK and AAPK Adsorbents

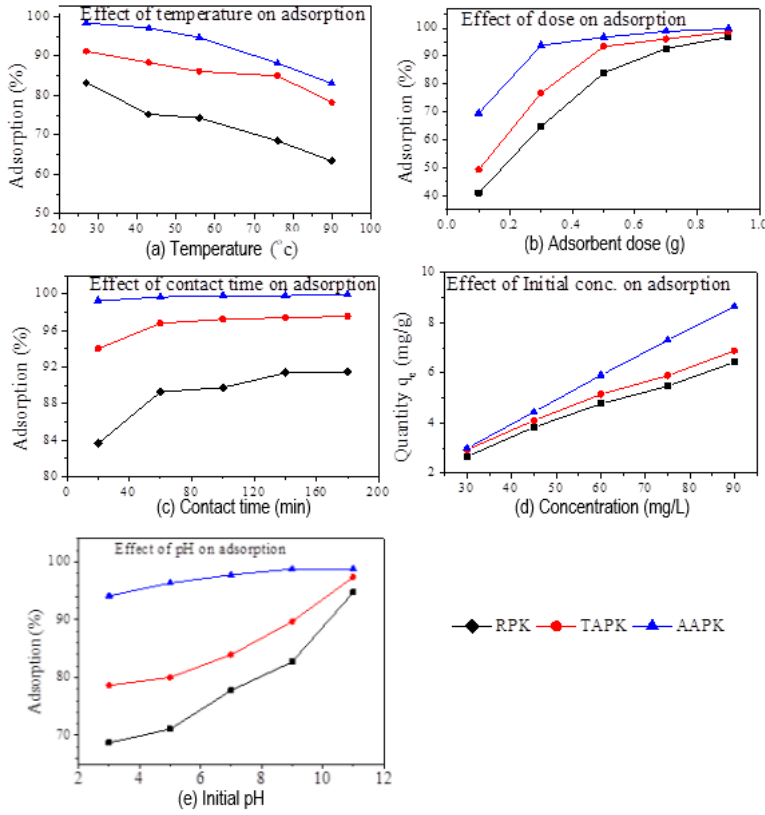


Figure 3
Effects of temperature, dose, contact time and initial concentration on adsorption

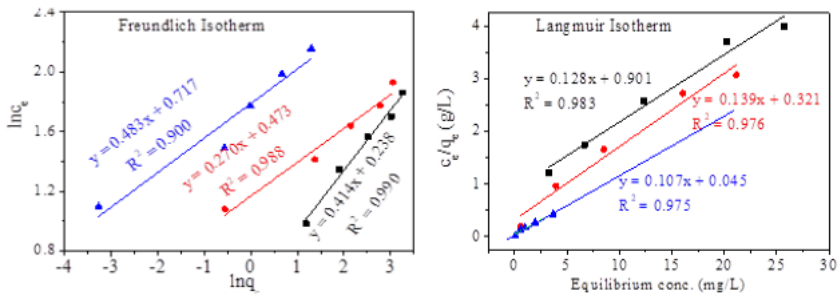


Figure 4
Adsorption Isotherms